Journal of the Brazilian Society of Mechanical Sciences and Engineering (2024) 46:209
https://doi.org/10.1007/s40430-023-04625-9

TECHNICAL PAPER

Numerical evaluation of the directed oil cooling system of a mobile power transformer

Luciene Martins Moura[1] · Rudolf Huebner[1] · Paulo Vinicius Trevizoli[1]

Received: 22 July 2023 / Accepted: 23 November 2023 / Published online: 14 March 2024
© The Author(s), under exclusive licence to The Brazilian Society of Mechanical Sciences and Engineering 2024

Abstract
Power transformers represent an important part of the capital investment in transmission and distribution substations. The cooling of the windings (electrical coil) depends on the convection of heat, enhanced by the forced circulation of oil through the windings and heat exchangers. The forced circulation of oil combined with the forced circulation of air in the heat exchangers is usually found in mobile transformers, whose compact structure is a challenge in terms of heat transfer rates. An improper design or fabrication problem associated with the assembling of the cooling system may result in an inefficient exchange of heat, which may lead to transformer failure from overheating or a reduction of the life span. In this context, the present work proposes a 2D mathematical model to simulate the winding cooling system of a 138 × 69–34 × 13.8 kV 25 MVA Mobile Power Transformer with the objective of investigating the causes of overheating. The model is implemented in CFD Ansys-Fluent® version 17.0 and validated with experimental data. It is evaluated the velocity and temperature distribution, and the identification of the hot spots on the transformer operating considering the nominal conditions for oil flow rate, inlet temperature, and power dissipated. The hot spot temperatures are compared with the current Brazilian Association of Technical Standards—NBR 5356-2: 2007 Power Transformers Part 2: Heating. After, some geometric and/or operational constraints are artificially imposed on the transformer. Their impact on the velocity and temperature fields, as well as the hot spot temperatures, are mapped in order to verify if they still respect the standard´s temperature limits and if imposed constraints may lead to the transformer failure. The numerical results clearly illustrate that geometric imperfections in the disks, guides, or axial cooling ducts have a direct impact on oil flow and temperature distributions. These imperfections can also alter the positioning and significantly increase the temperature of the hottest spot within the winding, sometimes even exceeding the requirements of the ABNT NBR 5356:2 standard in certain scenarios. Therefore, the proposed mathematical model serves as a valuable tool for investigating a complex and common issue within the energy distribution system. This issue not only inconveniences the population but also leads to economic challenges each year. Finally, the outcomes of this study can provide engineers with essential insights to enhance the thermal design of power transformers, as well it can assist in guiding maintenance efforts and understanding the root causes of new failures.

Keywords Power transformer · Oil cooling system · Overheating · Hot spot · CFD

1 Introduction

Power transformers immersed in naphthenic mineral oil represent the most common type in power distribution and transmission substations. The fluid has two main functions: dielectric and cooling. Interruptions in the power supply due to the failure have important technical and economic impacts related to costs of repair, non-transmitted energy, and all the inconveniences associated with industries and society. One of the most important parameters that govern the life expectancy of a transformer is its operating condition under loading (kA-kiloampères), that is,

Technical Editor: Guilherme Ribeiro.

✉ Luciene Martins Moura
lumoura@cemig.com.br

[1] Department of Mechanical Engineering, Federal University of Minas Gerais (UFMG), Belo Horizonte, MG 31270-901, Brazil

the power supplied to the power utility loads [1], which directly affects the oil temperature, windings and consequently, the insulating materials that compose it active part.

In case of failure of fixed transformers, mobile substations are normally employed for emergency assistance on the electrical system. The latter are, in general, compact units mounted on carts and made of insulating materials with high operating temperature limits and providing large power densities. Therefore, the cooling of this type of transformer is crucial, in which ineffective heat exchange can lead to overheating causing so-called hot spots inside the windings or in the magnetic core [2]. In high-power transformers (> 15 MVA), the temperature rise needs to be controlled to guarantee its proper operation and large lifespan.

There are different constructions of the cooling system in mobile transformers. The one of interest in this work is composed internally by a directed oil flow, established by centrifugal pumps associated with directing in ducts in the interior of the windings; and externally by forced air by using fans. This type of transformer is called oil directed air forced cooling (ODAF). The directed oil removes heat from the windings generated by Joule Effect and rejects it to the external environment throughout the heat exchanger, where the cold phase is the external forced air.

The evaluation of the cooling system of a power transformer is a current engineering problem that has been studied experimentally and numerically. During the last two decades, several authors have been using computational fluid dynamics (CFD), since it is a robust and reliable tool to investigate and to optimize thermofluid problems in power transformers. In the first decade, the main objective of CFD simulations was to determine the velocity and temperature fields of a winding in two-dimensional (2D) geometry immersed in a mineral oil [3, 4]. Recently, with the improvement of software, the use of three-dimensional models (3D) became possible, and allowed in depth studies in regard to the physical phenomena.

In 2009, Ortiz et al. [5] developed a mathematical model and performed CFD simulations using the software AnsysFluent®v6.1 to obtain the 3D representation of a 167 kVA dry-type transformer, along with an experimental method to evaluate the dissipation capacity in the electromagnetic circuit. In this model, only heat conduction was considered to evaluate temperature distribution. Fourteen thermocouples were installed between the high and low voltage windings and one thermocouple was placed on the magnetic core. The simulation results for the temperature distributions in the magnetic field of the core and in the windings were in agreement with the measured values. The authors suggest future works including the effects of heat transfer by radiation and an improvement of the proposed geometry.

Torriano et al. [6] and Quintela et al. [7] investigated the parameters that affect the temperature distribution in a disk-type transformer winding and performed simulations to calculate the mass flow rate and temperature distribution of a ONAN-type power transformer (Oil Natural convection Air Natural convection cooling). These authors used commercial packages, among them Ansys-Fluent®. They compared the simulations followed with experimental controls. In these experiments, controls were carried out in four different types of arrangement of the oil guides along the ducts formed in the windings. Initially, a distribution of uniform losses is applied, followed by non-uniform losses along the disks. The authors implement a three-dimensional representation using spatial subdivision of the domain of interest into a set of smaller elements, limiting the control volume and simplifying the elements that do not influence the flow. The results of the experiments demonstrated that a reduction in the number of guides along the winding would result in a poor distribution of oil flow in the radial pipelines. Thus, as the temperatures of the discs increase and stagnation of oil flow occurs in various pipelines. The computational simulations were more consistent to these experimental results when they were considered as flow rates and average temperatures defined as a boundary condition at the entrance of the pipelines.

Fonte et al. [8] also performed CFD simulations to analyze the fluid flow and heat transfer in a disc-type winding of a power transformer. The results provided detailed temperature and mass flow distribution along the windings, as well as the location and magnitude of the critical points. For a 2D axisymmetric model, the authors argue that the indirect effects of the spacers must be taken into account in the hydrodynamic and thermal simulations. In 3D simulations, a better agreement with experimental values was found. The deviations were attributed to uncertainties of the experiment itself, such as the measurements of temperatures at the inlet and outlet, or due to actual differences in the geometric parameters between model and equipment. The authors also concluded that CFD simulations may present more reliable results than experimental studies in reduced scale.

Tsili et al. [9] developed a 3D model of a transformer immersed in insulating oil, implemented via the finite element method, with the aim of studying the temperature distribution and the flow of insulating oil under different load conditions. The method was able to predict the temperature distribution of an ONAN type transformer. Similarly, Jarman et al. [10] developed a model implemented via the finite volume method in the commercial package Ansys CFX®. The numerical results were compared with experimental data from other authors [11] for the same type of transformer, and showed good agreement.

Campelo et al. [12] compared two different techniques, CFD and network hydraulic thermal modeling (NHTM), to

simulate the cooling system of core type transformers. The results for both were also compared with direct measurement data, using optical sensors and by thermoresistance, installed in an actual transformer. Both techniques were equally considered satisfactory, presenting very similar results, while some dispersions could be observed in respect to the experimental data. The authors attributed these differences to the systematic and random uncertainties of the measurements by sensor.

Daghrah [13] experimentally investigated the effects of a wide range of operational and geometric parameters on the fluid flow and temperature distributions of a disc-type transformer. His experimental setup enabled the adjustment of different parameters such as radial cooling duct height, axial cooling duct width, and number of discs per passage. Considering the Oil Direct (OD) cooling type, Daghrah experimentally validated some correlations derived from CFD simulations, using dimensional analysis under isothermal conditions. The dimensional analysis, regarding the oil flow rate and the pressure drop coefficient, was used to simplify the problem and determine the most influential dimensionless parameters that affected the oil flow distribution and the pressure drop in the windings. It was also verified that the dimensionless groups, such as the Reynolds number at the inlet and the ratio of the radial duct height to the axial duct width, can be correlated in the same way as the oil flow rate with the pressure drop coefficient, as in Zhang et al. (2018). On the other hand, under the non-isothermal conditions, it was found that the existence of electrical losses does not affect the mass flow distribution. Also, an increase in the oil velocity at the inlet of the duct may cause reverse flow and stagnation of the oil, and therefore, the temperature of the hottest point would not be reduced with the increase in the velocity at the inlet of the duct.

Santisteban et al. [14] employed two techniques, CFD and NHTM, to obtain mass flow, mean and hottest point temperatures of the winding in a disc-type power transformer. The results of both methods for ON and OD types of cooling systems were evaluated and compared. The models were also tested for three different fluids: mineral oil, natural ester and synthetic ester. For the three types of fluids, regardless of ON or OD cooling, the mass flow distributions through the radial channels, obtained in NHTM and CFD, were similar. Regarding the temperature distribution, the deviations between the two techniques were more significant but still considered acceptable in the range of operating temperatures.

In Daghrah et al. [2], a numerical study was developed to predict the temperature distribution in an ODAF type system. The results for flow and temperature fields were compared with experimental measurements from Daghrah [13]. It was observed that two-dimensional models are reliable when there are no significant reverse flows, and hence, three-dimensional models present results closer to the experimental ones in the presence of reverse flows.

In this context, Computational Fluid Dynamics (CFD) simulations showed to be quite reliable to predict the flow and temperature distributions in power transformers operating under nominal conditions. However, the open literature lacks sufficient information concerning how malfunctions and structural imperfections (non-nominal conditions) can result in inadequate heat transfer, and subsequently, the premature failure of transformers. This knowledge gap is particularly pronounced in the case of transformers with stringent volume and weight constraints, such as mobile substations. Consequently, the application of CFD simulations can be extended to encompass non-nominal conditions, enabling the evaluation of various scenarios and yielding valuable insights into the emergence of hot spots and early failure cases.

The present work proposes a 2D mathematical model for the flow of fluids and heat transfer to investigate the possible causes of early failure reported in a real mobile transformer ODAF-type 138 × 69-34x × 13.8 kV–25 MVA, named in this work as *TM1*. This equipment was manufactured in 2014, and the failure accident was reported in 2018. Along those years, the equipment was operated by Companhia Energética de Minas Gerais (CEMIG), in Brazil. The numerical implementation is developed in CFD Ansys-Fluent® version 17.0. The model is initially validated with experimental results obtained from Daghrah [13] for a similar equipment with the same cooling principle (ODAF), and a good agreement is observed in relation to the temperature ranges and distribution along the transformer discs. The validation and the mesh independence study were carried out based on the Grid Convergence Index (GCI) methodology in accordance to the American Society of Mechanical Engineers—ASME: V&V 20 Standard for Verification and Validation in Computational Fluid Dynamics and Heat Transfer (COMMITEE ASME, 2009).

After the validation, the *TM1* power transformer operating under nominal conditions is considered, and subsequently, eight different cases with non-nominal conditions are implemented and simulated. The proposed non-nominal conditions are related to operational and/or geometric variations from the manufacturer/catalog information. The non-nominal cases results for flow and temperature fields are compared to the nominal one, which enabled the observance of the hot spots with temperatures higher than those tolerated by insulating materials, in accordance with the Brazilian standard ABNT NBR 5356–16:2018. This allowed to evaluate the possibility of burnout and early failure.

2 Mathematical model

2.1 Model domain

Figure 1 presents a schematic drawing of the ODAF-type mobile transformer studied in this work. As in Fig. 1a, its active part has three columns (one per phase), each one with a coil of three windings: the low voltage winding (LV, number 6, in red), the high voltage (HV, number 5, in blue), and an additional winding (RHV, number 4, in white) responsible for regulating the voltage in the high voltage. The cooling oil enters the transformer through different inlets, positioned at the bottom, thus it is directed to the three individual columns and then to each winding, where it removes the generated heat (*Joule effect*). After leaving the transformer, the hotter oil flows through different components (compensation tank, servo valve, flow meter) returning to the centrifugal pump. The latter pumps the oil to the heat exchangers where it is cooled by the forced flow of external air, then the cooled oil finally returns to the transformer.

To simulate the whole domain (equipment) is computationally costly, being necessary to propose some simplifications. Starting from the geometry, it is assumed the following: (i) all external equipment (tubbing, compensation tank, servo valve, flow meter, pump and heat exchanger, among others) are neglected; (ii) the 3D domain is simplified to a 2D domain, as in Fig. 1b, where the radial (r) and axial (z) directions are considered; (iii) the winding are axis-symmetric; and (iv) to meet the objectives of this work, it is not necessary to simulate the three windings, and thus, only the HV winding is selected (see the control volume) to be investigated because several overheating accidents have been reported on it.

After applying (i) to (iv) the model domain is reduced to the one presented in Fig. 2. In Fig. 2a is shown the main parts of the winding including the oil inlet and outlet, Fig. 2b details the axial and the zigzag radial flows, and Fig. 2c illustrates the disc high (H_{disc}) and length (L_{disc}), the radial channel thickness (H_{ed}) and the axial channels thickness (L_{ce} and L_{cd}). The power transformer 138 × 69–34 × 13.8 kV–25 MVA comprises a magnetic iron (number 7, in Fig. 1a) core surrounded by co-axial disc type cylindrical windings.

The HV winding has a total of 96 discs (divided into two blocks, each one with 48 disks), axially separated by spacers stablishing the radial oil flow channels. The discs are made of copper, wrapped in Nomex410® paper. To conduct the flow throughout the radial ducts, flow guides (or washers) in Nomex are periodically inserted along the axial direction (see the black arrows in Fig. 2b). The entire winding is also involved in a cardboard, stablishing the axial flow channels. Table 1 shows the main dimensions of the HV winding in the in-study mobile power transformer, according to the Catalog of one of the manufacturers of this model [15].

2.2 Conservation equations

The fluid flow and heat transfer in the transformer winding are governed by conservation of mass, momentum and energy equations. In directed oil cooling, the effect of the buoyant force is negligible [2] and therefore fluid flow can be decoupled from heat transfer. Next are listed the simplifying hypotheses related to the fluid flow:

a. newtonian fluid;
b. steady state;
c. incompressible and laminar flow;
d. viscous dissipation and body forces are negligible;

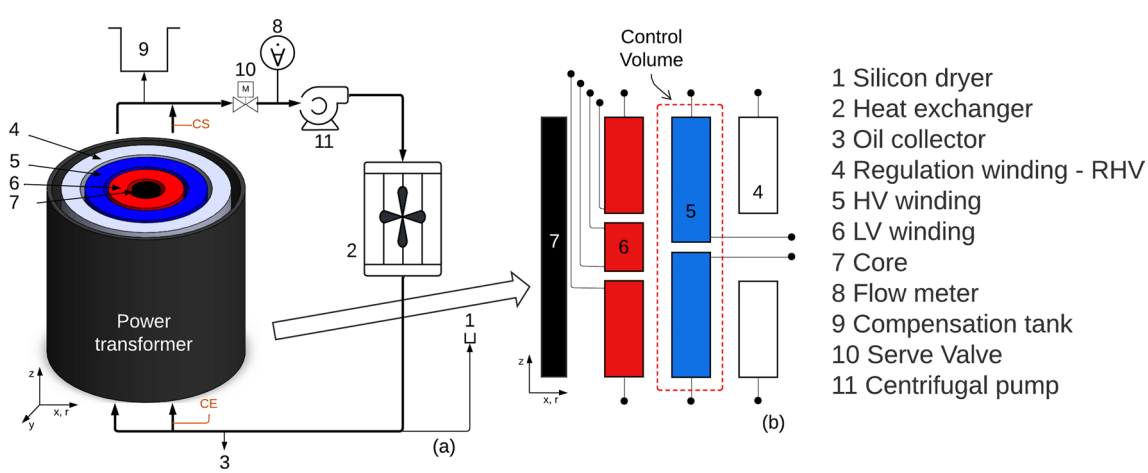

Fig. 1 ODAF-type power transformer: **a** schematic drawing of the complete equipment; **b** simplified 2D representation of the core and windings, as well the specification of the control volume

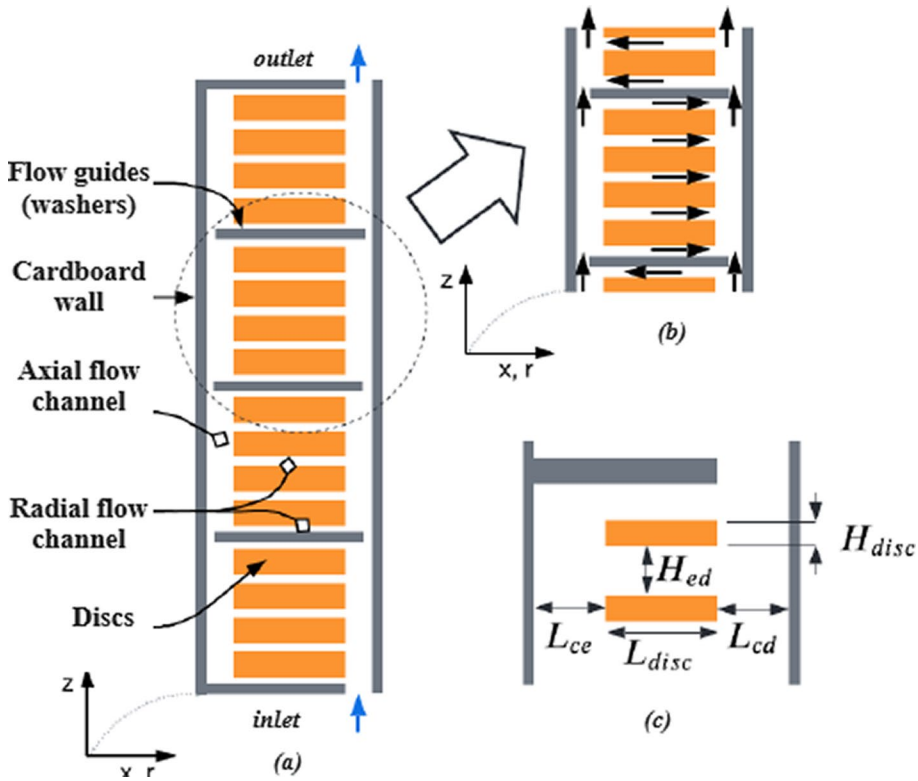

Fig. 2 Simplified 2D representation (model domain): **a** HV winding study domain; **b** expected axial and the radial flow along the HV winding; **c** details of the main dimensions

Table 1 Main dimensions and properties of the HV winding in the in-study mobile power transformer [15]

Variable		Dimension	Unit
Radial channel thickness	H_{ed}	4.00	mm
Rigth axial channel thickness	L_{cd}	7.00	mm
Left axial channel thickness	L_{ce}	8.00	mm
Distance between Nomex flow guides (whaser)	–	24.00	mm
Heigh of the Nomex flow guides (washer)	–	16.00	mm
Disc height	H_{disc}	9.58	mm
Disc length	L_{disc}	81.00	mm
Total disc heat transfer area	–	176,229	mm^2
Total of discs (divided into two blocs)	–	96	
HV winding internal diameter	–	637	mm
HV winding external diameter	–	799	mm
HV winding total height	–	1420	mm

e. the fluid properties are constant, except the viscosity and density that are temperature depend;
f. the solids (discs and walls) properties are constant;
g. the hydrodynamic and thermal effects of radial spacers (especially by reduction of cooling area) are not taken into account.

After applying these simplifications, the conservation equation to a 2D domain are as follows [16]. It is presented, respectively, the continuity equation (Eq. 1), the momentum (Navier–Stokes) equation in radial (r) direction (Eq. 2), the momentum (Navier–Stokes) equation in axial (z) direction (Eq. 3), and the energy equation for the fluid (Eq. 4) and solid (Eq. 5) phases of the domain.

$$\frac{1}{r}\frac{\partial(ru_r)}{\partial r}+\frac{\partial u_z}{\partial z}=0 \tag{1}$$

$$\rho_f\left(u_r\frac{\partial u_r}{\partial r}+u_z\frac{\partial u_r}{\partial z}\right)=\frac{\partial p}{\partial r}+\mu\left(\frac{\partial}{\partial r}\left(\frac{1}{r}\frac{\partial ru_z}{\partial z}\right)+\frac{\partial^2 u_r}{\partial z^2}\right) \tag{2}$$

$$\rho_f\left(u_r\frac{\partial u_z}{\partial r}+u_z\frac{\partial u_z}{\partial z}\right)=\frac{\partial p}{\partial z}+\mu\left(\frac{1}{r}\frac{\partial}{\partial r}\left(r\frac{\partial u_z}{\partial z}\right)+\frac{\partial^2 u_z}{\partial z^2}\right) \tag{3}$$

$$\left(u_r\frac{\partial T_f}{\partial r}+u_z\frac{\partial T_f}{\partial z}\right)=\frac{k_f}{\rho_f c_{p,f}}\left(\frac{1}{r}\frac{\partial}{\partial r}\left(r\frac{\partial T_f}{\partial r}\right)+\frac{\partial^2 T_f}{\partial z^2}\right) \tag{4}$$

$$\frac{1}{\rho_s c_{p,s}}(k_s\left(\frac{1}{r}\frac{\partial}{\partial r}\left(r\frac{\partial T_s}{\partial r}\right)+\frac{\partial^2 T_s}{\partial z^2}\right)+S_e)=0 \tag{5}$$

where u_r is the velocity along the radial direction, u_z is the velocity along the axial direction, ρ is density, p is pressure, μ is kinematic viscosity, T is temperature, k is thermal conductivity and c is specific heat. The source term (S_e) in

Table 2 Naphthenic oil properties [17]

Physical properties	Value or equation
ρ_f(kg/m^3)	$868(1-0.00064(T-20))$
μ(Pa s)	$5.73101-0.0612751T+0.000246719T^2-4.42934\times10^{-7}T^3+2.98939\times10^{-10}T^4$
k_f(W/(m K))	0.1278
c_f(J/(kg K))	2030

Eq. (5) represents the heat production per unit of volume due to the Joule effect. The subscripts f and s are related to fluid and solid properties, respectively. It is important to note that the viscous dissipation term for energy conservation is neglected because the oil velocity is small, and therefore, it can be considered negligible as in assumption (d). In addition, hypothesis (c) of laminar flow can be confirmed by evaluating the Reynolds number based on the hydraulic diameter and the oil average velocity.

The inlet boundary conditions are prescribed velocity u_{in} and oil temperature T_{in}, while at the outlet are uniform pressure profile at winding outlet (and inside the tank), $p_{\text{out}}=0$ and outlet flow $\left(\frac{\partial T}{\partial z}=0\right)$. See Fig. 2a for more details of the inlet and outlet. Also, at the wall, in the solid domain, for the conservation of momentum, it is considered the no-slip condition and the heat generated due to Joule effect ($\dot{Q}_0$) is also prescribed in accordance with the power transformer specifications, corresponding to total losses per disc.

2.3 Materials properties and operating conditions

The cooling and dielectric fluid used in the mobile power transformer 138 × 69–34 × 13.8 kV–25 MVA is a naphthenic oil, whose properties are presented in Table 2 [17]. For the temperature dependent properties, the presented equation used temperature in Celsius. The winding discs are composed of a group of copper conductors wrapped in Nomex410®, whose properties are presented in Table 3 [6]. The other solid properties are obtained from Ansys-Fluent®, version 17.0 (2017). In regard to the operating conditions considered in this work, they are shown in Table 4.

Table 3 Solid materials properties

Physical properties	Cooper wrapped in Nomex410 [7]	Cardboard AnsysFluent® 17.0, (2017)	Wood AnsysFluent® 17.0 (2017)
ρ_s(kg/m^3)	8978	930	700
k_s(W/(m K))	388.5	0.19	0.173
c_s(J/(kg K))	381	1340	2310

3 Numerical implementation

The mathematical model was implemented in Ansys-Fluent® version 17.0, as a 2D axisymmetric geometry. After defining the computational domain, several winding parameters are collected and represented in the module in CAD—D*esign Modeler*. It is necessary to characterize each region according to the types of domains: one for the fluid (isolated mineral oil); and three solid domains (disc, guides and spacers between blocks). In the *Solution Setup*, it is defined the properties of the materials, as in Table 2 for the cooling fluid, and Table 3 for the solids. In the copper disks of the windings, it is also necessary to enable the *Source Term* function as in Eq. (5), referring to the total losses (sum of losses in the core and in the windings). For the gradient calculations, the Least Square Cell Based or Cell-based Least Squares methods are used, while for the pressure term in the momentum equations, the Second Order scheme is selected, because it can provide greater accuracy compared to the Standard or Linear methods. For the advective terms in the momentum and energy equations, the *Second Order Upwind* interpolation function was selected. Finally, to solve the pressure–velocity coupling the *Coupled* method is selected. Table 5 briefly shows all the methods used as well the convergence criteria employed.

4 Results

4.1 Mesh size independence analysis and model validation

The mesh size independence analysis as well the model validation are carried out in accordance to the Grid Convergence

Table 4 Operating conditions

Variable		Units	Values/Ranges
Input flow velocity	u_{in}	m/s	0.4–0.7
Inlet temperature	T_{in}	°C	77.0
Disc losses[a]	$\dot{Q}_0$	W/m^3	3534.90

[a]The disc losses of 3534.90 W/m^3 is equivalent to 1 p.u. (system *per unit*) at the rated power of 25 MVA

Table 5 Solutions methods setup

Time	Steady
Energy	On
Flow models	Laminar
Pressure–velocity coupling method	Couple/pseudo transient
Discretization method	
Pressure	Second order
Momentum	Second order upwind
Energy	Second order upwind
Convergence criteria	
Continuity	0.000001
Speed x and y	0.000001
Energy	0.000001

Index methodology by ASME V&V20-2009 (COMMITEE ASME, 2009). To perform the validation, it is necessary to use a set of experimental data, however, there is no report of such information for the ODAF mobile power transformer 138 × 69–34 × 13.8 kV–25 MVA. On the other hand, Daghrah [12] presents several experimental data obtained from a directional oil system apparatus that reproduces, in reduced scale (50 W per plate, or equivalent of 2100 W/m^2), the operation of an ODAF transformer. The apparatus consists of a radiator, pump, flow meter and heating unit which imposes thermal losses as in a load winding, thus, similar to the ODAF system in this study.

This way, the 2D domain and the dimensions of the Daghrah [12] ODAF apparatus is implemented in the proposed model and simulations are performed, considering three different meshes called M1, M2 and M3 (in accordance with ASME V&V20-2009). In the fluid domain, it is considered structured meshes, while in the solid domain, an unstructured mesh of the triangular type was used. At the solid–fluid interface regions, the mesh inflation resource was used with the objective of improving the representation of the boundary layer and the velocity profile of fluid particles in this region. Mesh M1 is the most refined, with 1,112,532 elements and $h'_1 = 0.000225$ m; followed by mesh M2 with 511,793 elements and $h'_2 = 0.00045$ m; and M3 is the coarser with 138,392 elements and $h'_3 = 0.0009$ m. The refinement ratio (r) considered between the meshes are $r_{12} = r_{23} = 2$. Figure 3 presents the typical result for the temperature distribution along the winding (contours graphic) for mesh M2.

In these simulations, the operating conditions are $T_{in} = 55$ ºC, $u_{in} = 0.3$ m/s and $Q = 1$ p.u. Note that a prescribed loss unit represents the power dissipated at rated load taken with the base unit (W/m^3, see Table 4). This means that 1 p.u. is equal to 3534.90 W/m^3. The mesh independence study and model validation are based on the temperature elevation (δT_{HS}), calculated by Eq. (6), where T_{hs} is the temperature

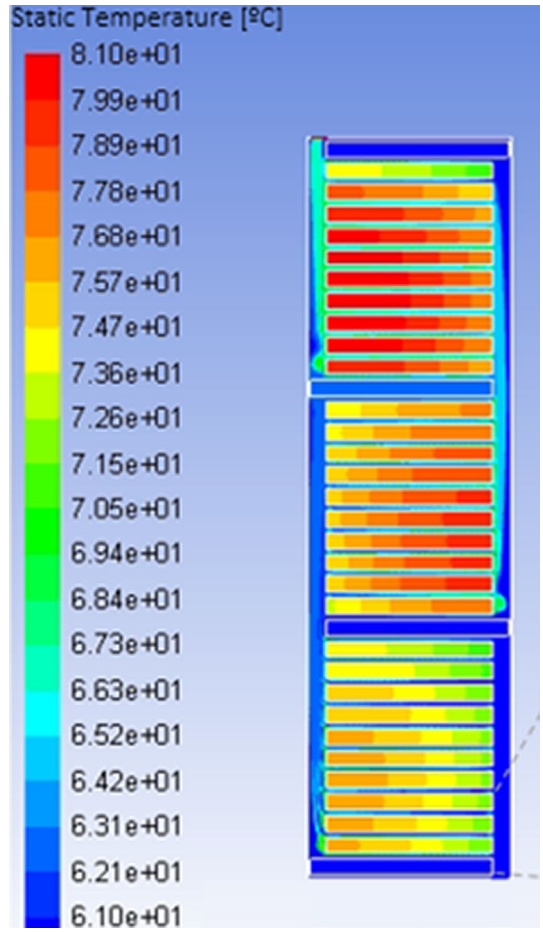

Fig. 3 Typical result for the temperature distribution along the winding

of the hottest spot at each disc, and e T_{in} is the inlet oil temperature. Therefore, δT_{HS} is evaluated along the discs (axial direction).

$$\delta T_{\mathrm{HS}} = T_{\mathrm{hs}} - T_{\mathrm{in}} \tag{6}$$

Figure 4 compares the simulation results for the distribution of δT_{HS} along the disks, for the three proposed meshes, with the experimental data from Daghrah [13]. First, it is noticeable the improvement to the numerical result when comparing meshes M3 and M2. It is also observed that both, meshes M2 and M1, guarantee a good reproduction of the experimental results, in terms of intensities of δT_{HS} and its distribution along the disks. In this case, the GCI obtained is 3.45% (ideally less than 5%), and thus, based on the ASME V&V20-2009, it can be stated that mesh M2 is refined enough to ensure the quality of the numerical results, as well that the proposed mathematical model can be considered as validated.

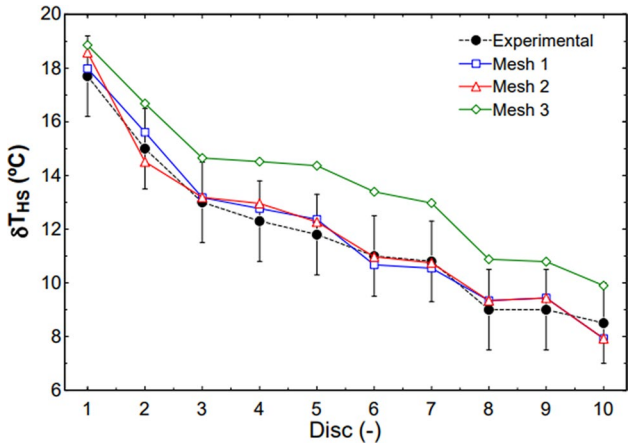

Fig. 4 Evaluation of the δT_{HS} values along the discs, comparing the meshes M1, M2 and M3 with the experimental data, for T_{in} = 55 ºC, u_{in} = 0.3 m/s and Q = 1 p.u

Following, in order to extend the validation of the mathematical model and the quality of mesh M2, it is performed novel simulations considering different operating conditions for inlet temperature, velocity and prescribed losses, all in accordance with the experimental data available in Daghrah [13], as summarized in Table 6. Figure 5 presents all the results, where: Fig. 5a is Validation 1, with T_{in} = 55 ºC, Fig. 5b is Validation 1, with T_{in} = 75 ºC; Fig. 5c is Validation 2, with u_{in} = 0.2 m/s; Fig. 5d is Validation 2, with u_{in} = 0.3 m/s; Fig. 5e is Validation 3, with Q_{disc} = 0.8 p.u.; and lastly, Fig. 5f is Validation 3, with Q_{disc} = 1.2 p.u.

Figure 5a and b compare the numerical results for the M2 grid with the experimental data considering two different inlet temperatures. A with good agreement is observed, with deviations smaller than 2 ºC in respect to the experiments. This attests that the model is sensible to inlet temperature shifting. Figure 5c and d used two different inlet velocities and, again, a good agreement is observed, with deviations smaller than 2 °C. Thus, the model is also sensible to inlet velocities variations. Finally, in Fig. 5e and f, two different prescribed losses are set, and the agreement is enhanced. Therefore, when varying the dissipated power, the numerical model is capable of reproducing the experimental values with good reliability.

Table 6 Operational conditions considered in the model validation

Case	Inlet temperature—T_{in} (ºC)	Inlet velocity—u_{in} (m/s)	Prescribed loss—Q_{disc} (p.u.)
Validation 1	55 and 75	0.3	1
Validation 2	60	0.2 and 0.3	1
Validation 3	60	0.3	0.8 and 1.2

In this context, the selected mesh M2 can be applied to the TM1 solution domain, which has dimensions as well some constructive and operational characteristics different from the experimental setup proposed by Daghrah [13]. The 2D domain is now made up of 96 disks, separated into two blocks of 48 each, which is discretized in a mesh of 1,560,496 elements applying the same specifications of the elements of mesh M2. Hence, the variations of the numerical solution obtained can be attributed to the geometric and operational conditions imposed on the transformer TM1 under study, as discussed next.

4.2 Nominal operating condition

The first simulation results for TM1 are regarded as normal operating conditions, considering that the assembly of the power transformer was flawless and the final product is exact as the designed one. Figure 6 shows the result for the disc-average temperature distribution along the axial direction, the points with a black solid square indicate the disks where the flow guides (or washers) are positioned along the winding. Figure 6a considers u_{in} fixed at 0.4 m/s; the oil inlet temperature at T_{in} = 77 °C and uniform energy loss equivalent to Q_{disc} = 3534.90 W/m^3 per disk, while Fig. 6b only shifts the u_{in} to 0.7 m/s.

From Fig. 6a and b, it can be seen that the highest temperatures are at the center of the coil, between discs 48 and 49, located at the end of block 1 and beginning of block 2, respectively. Notice that block 1, in general, has lower temperatures than those observed in block 2. This is because block 1 discs exchange heat with the oil at the lowest temperatures, while at block 2, the coolant oil is already warmed up from the heat gained from the discs in block 1. Comparing the results for the different velocities, some similarities are noted, but at u_{in} fixed at 0.7 m/s the average temperature is reduced from 89.1 °C (0.4 m/s) to 86.1 °C (0.7 m/s). Regarding the hottest spot, it remains on disk 48 to both conditions, while the hottest spot presents a lower temperature for 0.7 m/s case, at 89.5ºC, compared with 94.5 ºC for 0.4 m/s. As a conclusion, both cases meet the current Brazilian standard ABNT NBR 5356–16:2018, and there is no concern related to overheating of the power transformer, as well early failure, under the nominal operating conditions.

4.3 Non-nominal conditions

In this section, several non-nominal conditions and/or structural imperfections that supposedly can impact the thermal performance of an ODAF-type power transformer will be artificially imposed into the simulations. Notice that thermal performance is understood here as the capacity of the simulated power transformer to operate safely and stably

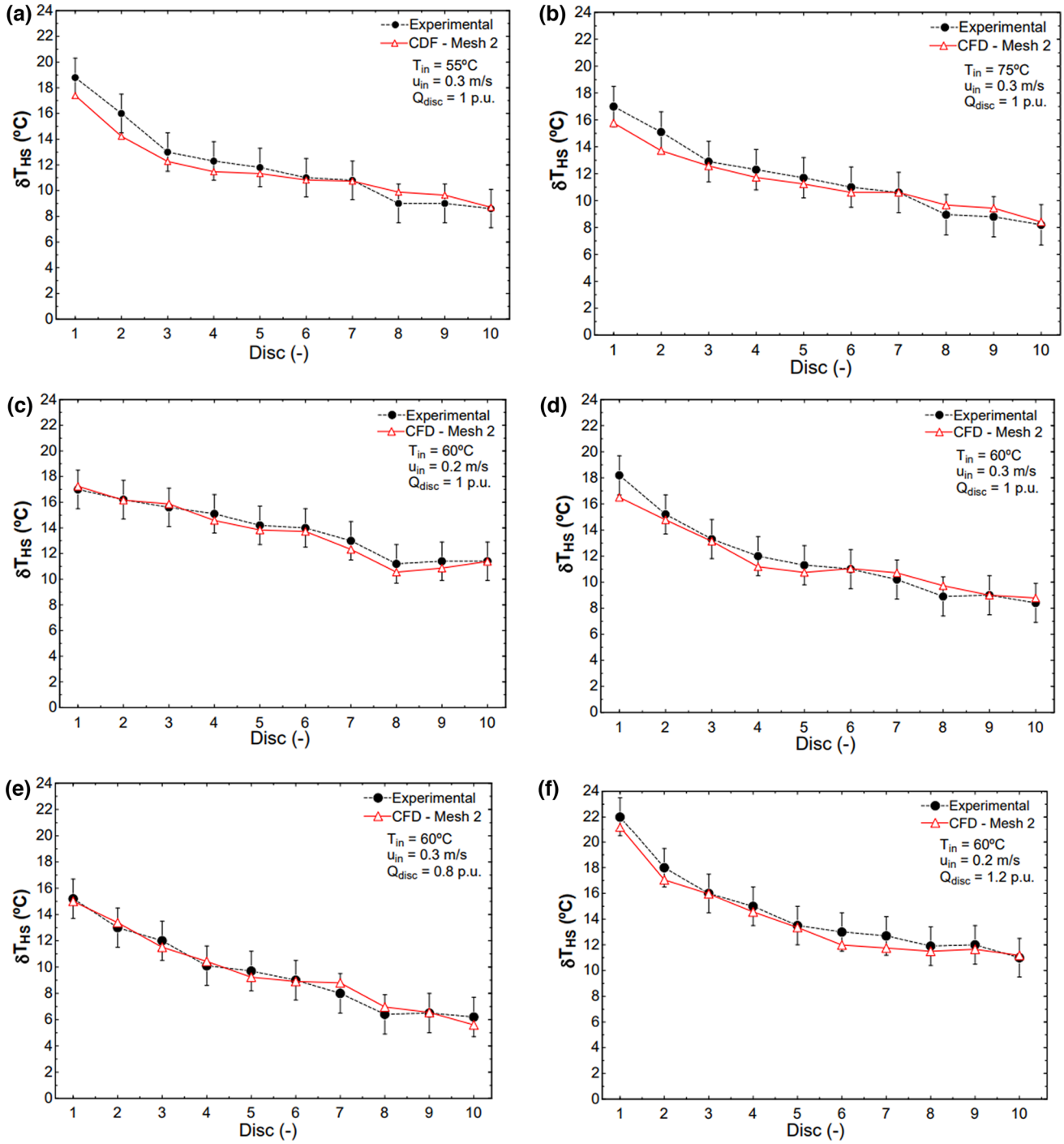

Fig. 5 Validation cases: **a** Validation 1 – T_{in} = 55 ºC, u_{in} = 0.3 m/s, Q_{disc} = 1 p.u.; **b** validation 1 – T_{in} = 75 ºC, u_{in} = 0.3 m/s, Q_{disc} = 1 p.u.; **c** Validation 2—T_{in} = 60 ºC , u_{in} = 0.2 m/s, Q_{disc} = 1 p.u.; **d** validation 2 – T_{in} = 60 ºC, u_{in} = 0.3 m/s, Q_{disc} = 1 p.u.; **e** Validation 3—inlet temperature 60ºC, u_{in} = 0.3 m/s, Q_{disc} = 0.8 p.u.; **f** Validation 3—inlet temperature 60ºC, u_{in} = 0.3 m/s, Q_{disc} = 1.2 p.u

according to the predicted rated capacities. In this sense, it is verified that the simulations carried out under nominal conditions and with input speeds of 0.4 and 0.7 m/s presented satisfactory thermal performance, compatible with the manufacturer's specifications and the current Brazilian standard. By imposing non-nominal conditions and/or structural imperfections, the temperature profiles are evaluated, as well as the intensity and location of the hottest spot, which makes possible to evaluate if there they can impact

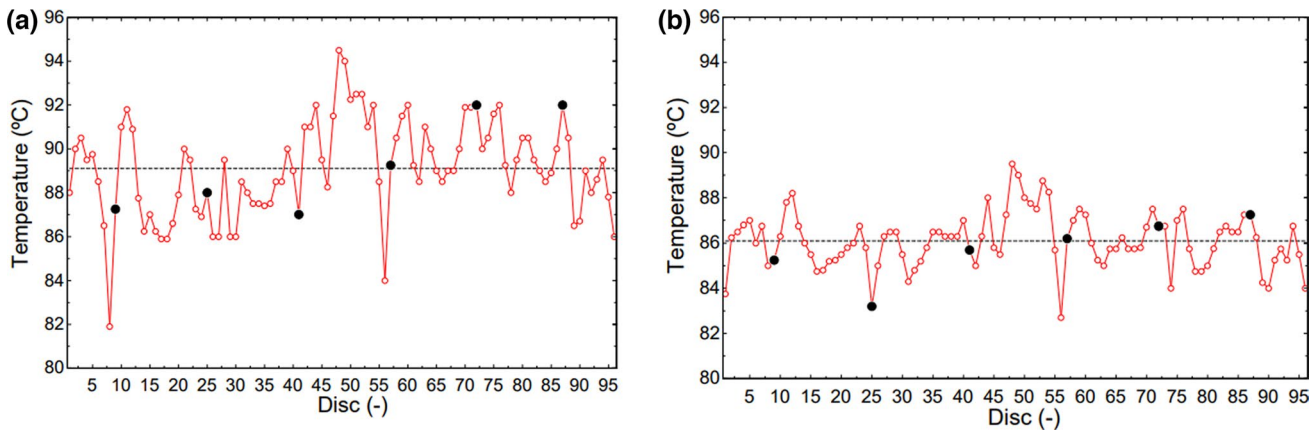

Fig. 6 Numerical results for the disc-averaged temperature distribution along the power transformer considering nominal conditions, where $T_{in} = 77$ °C, $Q_{disc} = 3534.90$ W/m^3 per disk, and: **a** $u_{in} = 0.4$ m/s; **b** $u_{in} = 0.7$ m/s

the thermal performance of the transformer, leading to overheating and early failure.

Based on field surveys and inspection performed on the actual TM1, ODAF-type power transformer, it was possible to assess that its failure initially occurred at the base of the first block of the winding, between disks 1 and 2. This delimited the envelope of possible non-nominal conditions and structural imperfections, which can impact on the fluid flow and heat transfer, leading to three fundamental assumptions:

i. ineffective thermal exchanges due to design or assembly imperfections, involving positioning of guides, covers, pressing rings or ducts;
ii. failures associated with the speed imposed at the entrance of the duct;
iii. non-uniform distribution of losses.

From these three assumptions, eight scenarios of geometric and operational deviations are elaborated. Depending on the case, the geometry is modified and the mesh rebuilt, and/or the initial input is changed, and a novel simulation is performed. The results of the non-nominal conditions are then compared with the nominal ones, and linked to common types of faults in transformer windings, especially the one observed at the TM1 under investigation.

Table 7 Summary of non-nominal conditions scenarios and simulation results in regard to the hot spot temperature (in ºC) and location (disc)

Simulated Condition	u_{in}(m/s)	Q_{disc}(p.u.)	Hot Spot (disc/ºC) (disc/°C)
Normal Operating condition	0.4	1	48/94.5
	0.7	1	48/89.5
i. Deformation of the oil guides	0.4	1	85/110.4
	0.7	1	72/97.1
ii. Displacement of the discs	0.4	1	87 /120.9
	0.7	1	87/104.6
iii. Obstruction of the inlet	0.4	1	84/119.9
	0.7	1	85/103.0
iv. Obstruction of the outlet	0.4	1	85/107.7
	0.7	1	85/90.2
v. Displacement of the base cover	0.4	1	85/98.8
	0.7	1	88/87.8
vi. Combined effects of disc displacement and reduced speed	0.3	1	93/122.5
vii. Combined effects of displacement of the base cover and reduced speed	0.3	1	83/134.9
viii. Non-uniform losses along the windings	0.4	1–5	2/124.4
	0.7	1–5	2/118.0

The proposed scenarios are: (i) deformation of the oil guides; (ii) displacement of the discs; (iii) obstruction of the inlet; (iv) obstruction of the outlet; (v) displacement of the base cover; (vi) combined effects of disc displacement and reduced speed; (vii) combined effects of displacement of the base cover and reduced speed; (viii) non-uniform losses along the windings. Table 7 presents a summary of these conditions imposed in each scenario and simulation results for the location and intensity of the hot spot. All the simulations considered the inlet oil temperature of $T_{in} = 77$ °C.

When analyzing the results, it is clear that the restrictions imposed on the oil flow (scenarios i to vii) affects the performance, especially at the lower flow rates. Let us evaluate in more details one of those scenarios: (i) the deformation of the oil guides. This condition was evidenced at the investigative inspections when the active part of the TM1 was disassembled. The correct positioning of the oil guides is essential to ensure the proper circulation of oil along the winding ducts and to limit the speed of oil passage as demonstrated by Yaqoob [18] and Zhang et al. [19].

Figure 7 presents the velocity fields under nominal conditions and scenario (i). Figure 7a is the nominal at 0.4 m/s inlet velocity, with streamlines simulations; Fig. 7b is the nominal at 0.7 m/s, with streamlines simulations. Observing the velocity vectors, it is also verified that there are regions where the oil flow reaches 0.94 m/s, values very close to the limit recommended by IEEE 1538 (2000) [20], this is, lower than 1.0 m/s. Figure 7c is scenario (i) at 0.4 m/s, here it is possible to identify the most critical regions that are at the base of the winding: (1) close to the entry; (2) between the first 8 disks; and (3) the right vertical duct. Note that there are regions where the oil flow reaches 0.79 m/s. In turn, in Fig. 7d, for an input of 0.7 m/s, there are regions with values above this limit, reaching approximately 1.3 m/s, which does not occur in the nominal conditions. These results justify the manufacturer's recommendations to limit the inlet velocity up to 0.7 m/s. The extrapolation of the flow velocity limit

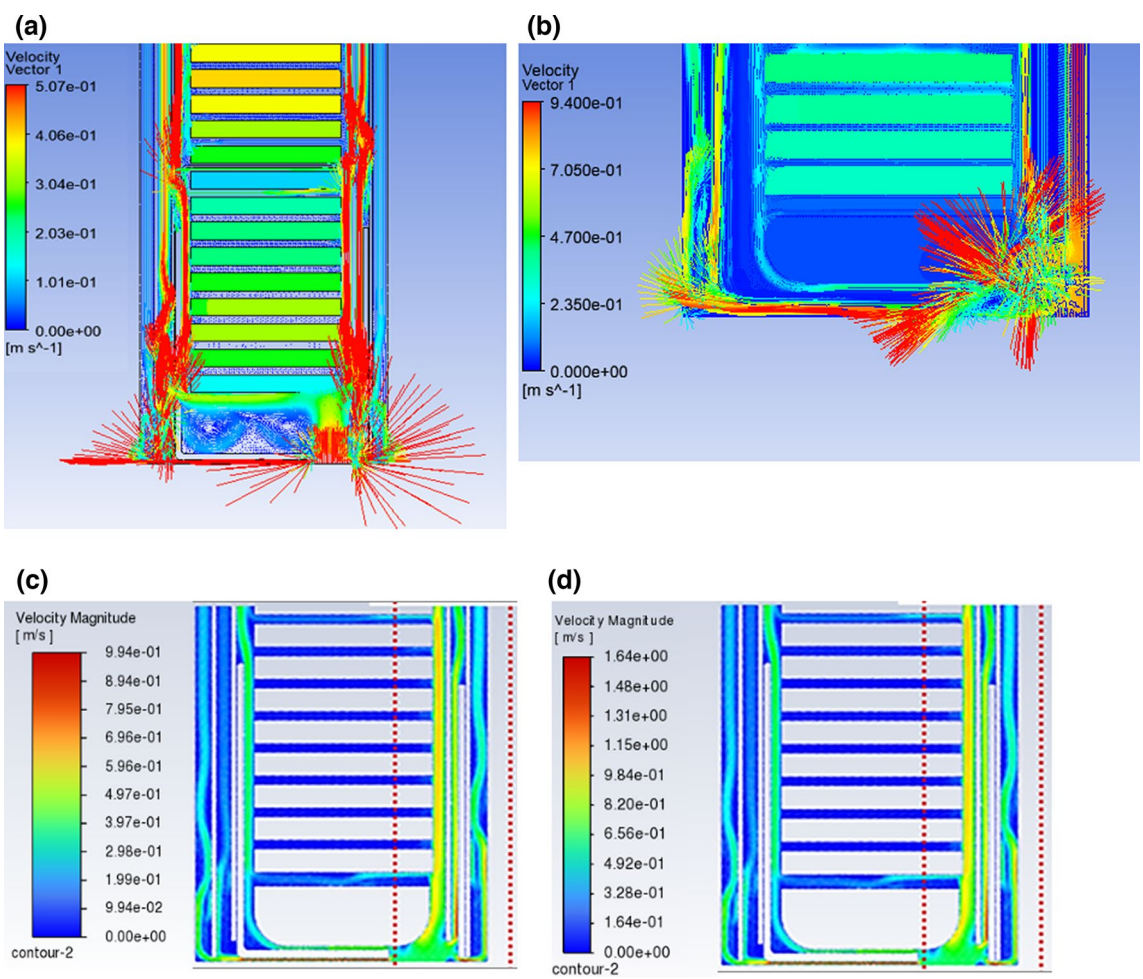

Fig. 7 Simulation velocity fields results, inlet region: **a** nominal conditions with streamlines and $u_{in} = 0.4$ m/s; **b** nominal conditions with streamlines and $u_{in} = 0.7$ m/s; **c** scenario (i) and $u_{in} = 0.4$ m/s; **d** scenario (i) and $u_{in} = 0.7$ m/s

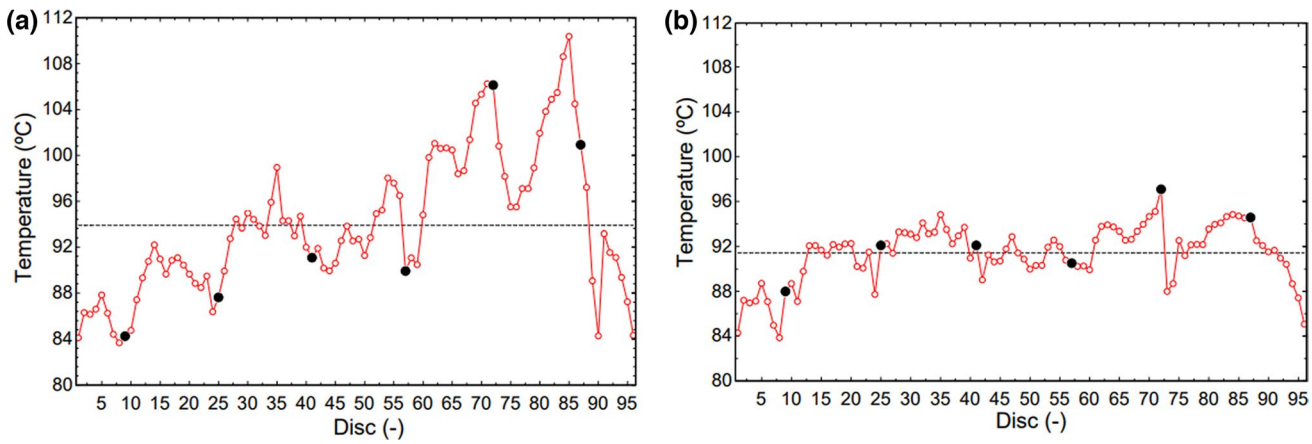

Fig. 8 Numerical results for the disc-averaged temperature distribution for scenario (i): **a** u_{in} = 0.4 m/s; **b** u_{in} = 0.7 m/s

may lead to an increase in the Electrostatic Charging Tendency—ECT, as studied by Shimizu et al. [21], Bustin and Dukek [22] and Cesar et al. [23]. Although it is not evaluated in this study, the ECT should be considered as a factor of risk for failures in speed control between the channels inside the coils.

Figure 8 shows the disc-averaged temperature distribution along the axial direction for scenario (i) at u_{in} = 0.4 m/s and u_{in} = 0.7 m/s, Fig. 8a and b, respectively. Comparing Figs. 8 and 6 (nominal conditions) it is clear how the imposed flow restriction impacts the temperature distribution. It is no longer close to a uniform distribution as observed in Fig. 6, presenting lower temperature regions (initial discs—from 1 to 10 in Fig. 8a) and higher temperature regions (from 67 to 87 in Fig. 8a). Finally, as already presented in Table 6, the hot spot temperature also rose from 94.5 to 110.4ºC as well its location changed from disc 48 to 85, for 0.4 m/s. A similar result is observed for 0.7 m/s.

Certainly, the cooling system was not designed to operate at this temperature distribution as well at such intensity of the hottest spot. If scenario (i) is combined with any other imperfection or malfunction, the fluid flow and heat transfer can be even more impacted leading to overheating and early failure. See Table 6, scenario (vi) and (vii), how combining two different effects impacts the hot spot temperature and location if compared with nominal conditions or scenarios (ii) and (v).

Even though scenarios (i) to (vii) lead to results that may impact on fluid flow and heat transfer of the oil directed cooling system, presenting inconsistent flow patterns, temperature profiles and higher temperatures of the hottest spot, they do not explain the cause of the early failure in the investigated TM1 ODAF-type power transformer, this is, at the first two discs. Next it is evaluated scenario (viii) of non-uniform losses distribution along the disks. This enables to simulate a local failure that reproduces the thermal effect on the disks from the introduction of a short circuit, which may result from mechanical effort, breaking of spacing between discs or insulating materials. IN this context, it is assumed that in the region of discs 1 and 2 there is a non-uniformity in terms of losses and the prescribed value of $Q' = 5$ p.u. (simulating an I_{cc} of 2.25 p.u.) is imputed. This condition

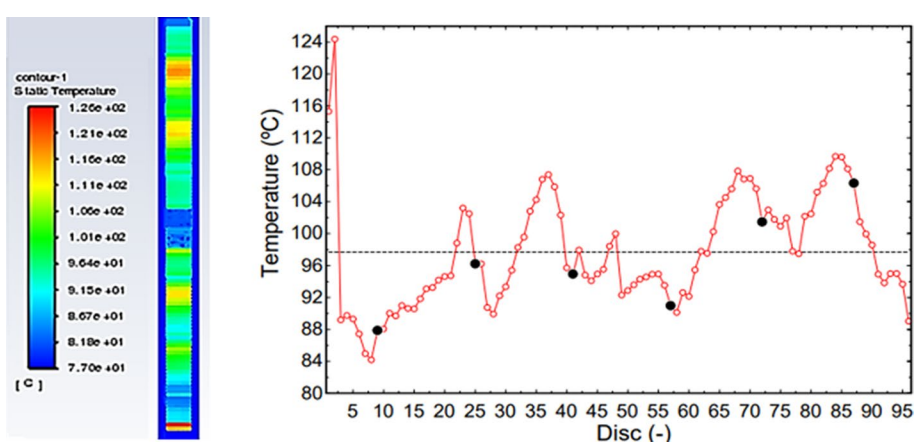

Fig. 9 Numerical results for the disc-averaged temperature distribution for scenario (viii), where u_{in} = 0.4 m/s; and T_{in} = 77 ºC

would be endurable by the equipment for just over 1 min. On the other disks is maintained the prescribed value of $Q' = 1$ p.u. Figure 9 shows the results for scenario (viii), considering $u_{in} = 0.4$ m/s and the inlet oil temperature of 77 ºC.

It is verified that a severe rise on the temperature of disk 2 achieving 124.38 °C, while in disk 1 the temperature is 115.31 °C. Therefore, these results indicate that a short circuit between turns, even at low currents (which can be sustained for a longer time, when compared to short currents of high intensity for a very short period) can explain the occurrence of the under investigation accident in TM1 power transformer. In this way, the equipment would be subjected to non-uniform losses in the region of disks 1 and 2, resulting in its early failure.

5 Conclusions

The occurrence of accidents in power transformers causes several social and economic disorders every year. One of the main causes of accidents is the improper heat transfer in the windings. The object of study in this research, the early failure in the mobile power transformer (TM1), was registered in 2018, while it was manufactured in 2014. During those years, the equipment was operated by Companhia Energética de Minas Gerais (CEMIG), in accordance with the current legislation. Additionally, in 2019, novel failures were reported in other power transformers (different units) of the same model and year of manufacture. This way, failures associated with preventive maintenance or operational issues were disregarded, especially if one considers that these power transformers burned out before the minimum time recommended by the manufacturers for interventions, which is 6 years at nominal load. Also, in accordance with the technical reports, semiannual predictive maintenance, such as oil chromatography, did not show gradual evolution of gasses, such as acetylene. So that an investigation in regard to the possible causes of the ineffective heat transfer is of great value in preventing future incidents.

In this context, this work developed a mathematical model to study the fluid flow and heat transfer in a ODAF-type cooling system, part of a mobile power transformer. The bidimensional and steady-state model was implemented in CFD software Ansys-Fluent® version 17.0. It was submitted to a mesh size independence analysis and validation in accordance with the GCI methodology. For the validation, it was used the experimental data by Daghrah [12] obtained from an experimental apparatus that emulates a similar ODAF transformer. A very good agreement for the disk-averaged temperature distribution along the windings was observed, as well GCI of 3.45% was obtained. In addition, several input conditions were changed to a more in-depth validation of the model.

After the validation, several simulations were performed and the following conclusions were obtained:

- When considering nominal operating conditions, the disk-averaged temperature distribution along the winding can be considered close to be uniform, as well the hottest spot temperature is in accordance with the current Brazilian standards ABNT NBR 5356-16:2018. Hence, there was no reason to cause an early failure.
- When considering geometric imperfections and/or non-nominal conditions, it was notorious a disturbance of the disk-averaged temperature distribution as well the impact on the hottest temperature intensity and location, which may cause local overheating above the admissible limits for the materials used in the insulation.
- Scenarios (i) and (viii) presented conditions that may impose a greater risk of failure between disks 1 and 2, which may be associated with the early failure identified in TM1. This is due to the extrapolation of the oil speed limits in this inlet region and the limits of temperature imposed by a non-uniform distribution of losses, caused by a possible dispersion of electromagnetic flux or a short circuit between turns.

Therefore, the proposed validated mathematical model and the in-study scenarios for geometric imperfections and non-nominal conditions proved to be a reliable tool for understanding the thermal behavior and the location of the hot spot, and can be applied by utilities, manufacturers and insurers. Moreover, other failures in ODAF-type transformers can be clarified, once the particularities of each transformer are implemented. As future stages of the research, it is intended to expand the analysis involving all the three windings, Low Voltage, High Voltage and Regulation, as well expanding the model to a 3D domain, including transient effects of electrical origin, electromagnetic and thermal coupling model.

References

1. Hamza S, Herskind T (2019) Dynamic thermoelectric modelling of oil-filled. In: Transformers for optimized IEEE Institute Of Electrical And Electronic Engineers. IEEE 1538:2000. Guide For Determination Of Maximum Winding Temperature Rise In Liquid Filled Transformers, 2000
2. Daghrah M, Wang Z, Zhongdong W, Qiang L, Jarman P, Walkerb D (2020) Flow and temperature distributions in a disc type winding-Part I: forced and directed cooling mode. Appl Thermal Eng, 165
3. Radakovic ZR, Sorgic MS (2010) Basics of detailed thermal-hydraulic model for thermal design of oil power transformers. IEEE Trans Power Delivery 25:790–802

4. Torriano F, Picher P, Chaaban M (2012) Numerical investigation of 3D flow and thermal effects in a disc-type transformer winding. Appl Thermal Eng, 40
5. Ortiz C, Skorec AW, Lavoie M, Benard P (2009) Parallel CFD analysis conjugate heat transfer in a dry-type transformer. IEEE Trans Industry Appl 45:1530–1534
6. Torriano F, Chaaban M, Picher P (2010) Numerical study of parameters affecting the temperature distribution in a disc-type transformer winding. Appl Therm Eng, 30
7. Quintela B, Torriano F, Campelo HM, Labbéa PM, Pichera P (2018) Numerical and experimental thermal fluid investigation of different disc-type power transformer winding arrangements. Int J Heat Fluid Flow
8. Fonte CM, Lopes JC, Dias MM, Sousa RG, Campelo HM, Lopes RC (2011) CFD Analysis of Core Type Power Transformers. In: 21st international conference on electricity distribution. Frankfurt 6–9, June 2011.
9. Tsili MA, Amoirales EI, Kladas AG, Souflaris AT (2012) Power transformer thermal analysis by using an advanced coupled 3D heat transfer and fluid flow FEM model. Int J Thermal Sci 53:188–201
10. Jarman P, Zhang X, Daghrah M, Liu Q, Wang Z, Dyer P, Gyore A, Smith, P, Mavrommatis P, Negro M (2012) Prediction of the oil flow distribution in oil-immersed transformer windings by network modelling and computational fluid dynamics. IET Electric Power Appl
11. Haritha VS, Rao TR, Amit J, Rammamorty M (2009) Thermal modeling of electrical utility. In: Third international conference on power systems, Kharagpur, India, 27–29 Dec 2009
12. Campelo HMR, Fernandez XL, Picher P, Torriano F (2013) Advanced thermal modelling techniques in power transformers. Review and Case Studies. ARWTR2013—Advanced Research Workshop on Transformers, Baiona, October 2013
13. Daghrah M (2017) Experimental study of transformer liquid flow and temperature distributions. Thesis (The Degree of Master), The University of Manchester
14. Santisteban A, Ortiz F, Carlos JR, Perez S, Mendez C, Fernández CD (2019) Thermal modeling of power transformer with different dielectric liquids. XI National and II International Engineering Thermodynamics Congress—2019. Responsibility Notice.
15. WEG (2020) Manufacturer's catalog—design review: remote controlled regulator transformer
16. Picher P, Torriano F, Chaaban M, Gravel S, Rajotte C, Girard B (2010) Optimization of transformer overload using advanced thermal modelling. CIGRÈ Session, Paris
17. Nynas AB (2014) Product Data Sheet: Nytro 11GBX-US, 2014.
18. Yaqoob MT (2013) Transformer thermal model of the disk coils with non directed oil flow. Masters thesis, Universiti Tun Hussein Malaysia
19. Zhang X, Wang ZD, Liu Q (2017) Interpretation of hot spot factor for transformers in OD cooling modes. IEEE Trans Power Delivery
20. IEEE Institute of Electrical and Electronic Engineers. IEEE 1538:2000. *Guide for determination of Maximum Winding Temperature Rise in Liquid Filled Transformers*, 2000.
21. Shimizu S, Murata H, Honda M (1979) Electrostatic in power transformer. IEEE Trans Power Apparatus Syst Pas-98(4)
22. Bustin WM, Dukek WG (1983) Eletrostatic hazards in the petroleum industry. Research Studies Press Ltd. England
23. Cesar LC, Vieira S, Sens MA, Marins LE, Fernandez JB (1989) National Seminar on Production and Transmission of Electric Energy, Curitiba

Publisher's Note Springer Nature remains neutral with regard to jurisdictional claims in published maps and institutional affiliations.

Springer Nature or its licensor (e.g. a society or other partner) holds exclusive rights to this article under a publishing agreement with the author(s) or other rightsholder(s); author self-archiving of the accepted manuscript version of this article is solely governed by the terms of such publishing agreement and applicable law.